AGU PUBLICATIONS

Geophysical Research Letters

RESEARCH LETTER
10.1002/2015GL065088

Key Points:
- Large deep-focus earthquakes have exhibited strong and unexpected seasonality
- The seasonality appears strongest in the northwest Pacific and South American subduction zones
- We make a testable prediction of seasonality in future large deep earthquakes

Supporting Information:
- Figures S1–S4 and Table S1

Correspondence to:
Z. Zhan,
zwzhan@gps.caltech.edu

Citation:
Zhan, Z., and P. M. Shearer (2015), Possible seasonality in large deep-focus earthquakes, *Geophys. Res. Lett.*, *42*, 7366–7373, doi:10.1002/2015GL065088.

Received 24 JUN 2015
Accepted 19 AUG 2015
Accepted article online 21 AUG 2015
Published online 16 SEP 2015

Possible seasonality in large deep-focus earthquakes

Zhongwen Zhan[1,2] and Peter M. Shearer[1]

[1]Scripps Institution of Oceanography, University of California, San Diego, La Jolla, California, USA, [2]Now at Seismological Laboratory, California Institute of Technology, Pasadena, California, USA

Abstract Large deep-focus earthquakes (magnitude > 7.0, depth > 500 km) have exhibited strong seasonality in their occurrence times since the beginning of global earthquake catalogs. Of 60 such events from 1900 to the present, 42 have occurred in the middle half of each year. The seasonality appears strongest in the northwest Pacific subduction zones and weakest in the Tonga region. Taken at face value, the surplus of northern hemisphere summer events is statistically significant, but due to the ex post facto hypothesis testing, the absence of seasonality in smaller deep earthquakes, and the lack of a known physical triggering mechanism, we cannot rule out that the observed seasonality is just random chance. However, we can make a testable prediction of seasonality in future large deep-focus earthquakes, which, given likely earthquake occurrence rates, should be verified or falsified within a few decades. If confirmed, deep earthquake seasonality would challenge our current understanding of deep earthquakes.

1. Introduction

The solid Earth is continuously perturbed by periodic stresses from solid Earth tides, ocean tides [*Agnew*, 2007], and surface loads (e.g., snow, glaciers, and atmosphere) [*Wahr et al.*, 1998]. Correlation of earthquake activity with one or more tidal frequencies would have important implications for earthquake nucleation and prediction. However, numerous attempts to find such correlations have yielded mixed results [*Heaton*, 1975; *Vidale et al.*, 1998; *Cochran et al.*, 2004; *Ader and Avouac*, 2013] and apparent observations of earthquake periodicity often prove unreliable after more careful statistical tests [*Jeffreys*, 1938; *Heaton*, 1982]. The difficulty in identifying a correlation often arises from two problems: (a) Spatial and/or temporal clustering of earthquakes (e.g., aftershocks) can bias statistical tests that assume independence of event occurrence [*Jeffreys*, 1938; *Heaton*, 1982; *Shearer and Stark*, 2012] and (b) data fishing issues; i.e., statistical tests are applied only after recognizing a "periodic" pattern [*Shearer and Stark*, 2012; *Gelman and Loken*, 2014; *Nuzzo*, 2014]. These types of problems are common not only in statistical seismology but also in many other fields.

Among the studies searching for earthquake periodicity, events deeper than 70 km (hereafter termed deep earthquakes), especially those deeper than 300 km (hereafter termed deep-focus earthquakes), have often drawn special attention [*Conrad*, 1933; *Stetson*, 1935; *Landsberg*, 1948; *Curchin and Pennington*, 1987]. Although deep earthquakes are rarer than shallow events and have enigmatic mechanisms, their relatively impulsive and clean seismic waveforms have led to the perception that the deep earthquake environment may be more homogeneous than that of shallow earthquakes and hence more susceptible/vulnerable to periodic stress loading at small amplitudes. In 1933, *Conrad* [1933] reported that deep earthquakes are more likely to occur in summer, and several papers in the 1930s reported similar observations [*Frohlich*, 2006]. However, later, more careful statistical studies using better data sets failed to confirm this seasonality, and the two statistical problems mentioned above started to be recognized [*Jeffreys*, 1938; *Heaton*, 1982]. For a good review of this history see section 5.2 of Frohlich's review book "Deep Earthquakes" [*Frohlich*, 2006].

Here we report new possible evidence for deep-focus (depth > 300 km) earthquake seasonality. Specifically, we find that from 1900 to the present large ($M > 7.0$) deep-focus earthquakes have occurred 2 to 3 times more often in the middle half of each year, i.e., Northern Hemisphere summer time. While naive application of standard statistical tests would suggest that this is unlikely to be due to random chance, any hypothesis tests are based on observations that have already occurred; i.e., the fundamental data fishing problem cannot be circumvented. Nonetheless, we still consider it useful to report our observations in order to stimulate broader investigations (seismological or statistical). In the end, we make a testable prediction of future large deep earthquake behavior based on past observations of deep-focus earthquake seasonality.

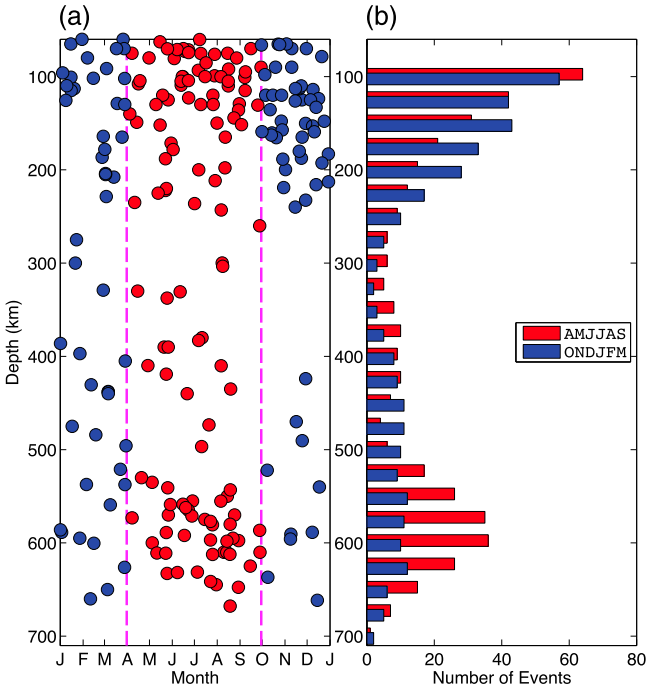

Figure 1. Seasonal pattern of large ($M_w \geq 7.0$) deep earthquakes (depth $>$ 70 km) from 1900 to the present. (a) Earthquake depths versus month of occurrence, from January (J) to December (D). Events in the middle half of each year (from 1 April to 1 October, called summer) are colored in red; and those in the other half (called winter) are colored in blue, divided by the two dashed lines. While at most depth ranges event depths do not correlate with month, a cluster in summer appears for events deeper than 500 km. (b) Depth histograms for events in summer and winter, respectively, in red and blue. Each bin represents the number of events within a 100 km depth range around the centers, which are spaced every 10 km. Below 500 km depth, 2 to 3 times more events occurred in summer (AMJJAS) than in winter (ONDJFM).

2. Observations

The earthquake catalog used in this study is the International Seismological Centre-Global Earthquake Model (ISC-GEM) Global Instrumental Earthquake Catalogue from 1900 to 2009 [*Storchak et al.*, 2013], complemented by the Global Centroid Moment Tensor (CMT) catalog from 2009 to 2014 [*Dziewonski et al.*, 1981; *Ekström et al.*, 2012]. The ISC-GEM catalog is compiled for the purpose of assessing seismic hazard and involves special efforts to relocate and provide more consistent magnitudes (e.g., with the Global CMT catalog). For deep earthquakes (depth $>$ 70 km), the ISC-GEM catalog is complete down to $M_w \sim 6$, although the first 30 years are probably more questionable [*Michael*, 2014]. The Global CMT catalog is complete down to M_w 5.5 for deep earthquakes. These two catalogs have relatively consistent magnitudes and depths. Figure 1a plots all $M_w \geq 7.0$ deep earthquake depths versus month of occurrence. For simplicity, we call the middle half of the year (from 1 April to 1 October) "summer," colored in red, and call the other half of the year "winter," colored in blue. If there is no seasonality in deep earthquake occurrence, we expect to see no correlation between event depth and month, which is indeed what we observe for most depths. However, for depths larger than 500 km, there is a cluster of events in summer months (red dots), with higher apparent density than in winter (blue dots). To confirm this difference, we create a histogram of the events as a function of depth, separately for summer (red bars) and winter (blue bars) events (Figure 1b). Each bin represents the number of events within a 100 km depth range around the bin centers, which are spaced every 10 km; i.e., neighboring depth windows have significant overlap. From this figure, it is clear that below 500 km depth, 2 to 3 times more events occurred in summer (April–September (AMJJAS); red) than in winter (October–March (ONDJFM); blue).

A double-mode depth distribution of global seismicity has been recognized for a long time [*Frohlich*, 2006; *Houston*, 2007; *Green et al.*, 2010]. The earthquake rate peaks near the surface, decays rapidly with depth, reaching a minimum at about 300–400 km, and then increases to a second peak at about 600 km, before terminating sharply near the 670 km discontinuity. For large deep earthquakes in Figure 1b, we notice that the summer seismicity displays a very similar double-mode distribution, while the winter seismicity in blue is almost flat below 400 km and does not have the second mode. As a result, the difference between summer and winter is greatest below 500 km, near the second peak.

Interestingly, the seasonality seems to only exist for deep-focus earthquakes larger than magnitude 7.0. In a similar plot as Figure 1 but for events with M_w between 6.5 and 7.0 (Figure S1a in the supporting information), winter and summer have very similar double-mode distributions and the difference in their numbers is small. Note that Figures 1 and S1a show somewhat opposite behavior between summer and winter events; if we sum them as in Figure S1b, for all magnitudes larger than 6.5, the surplus of summer events below 500 km

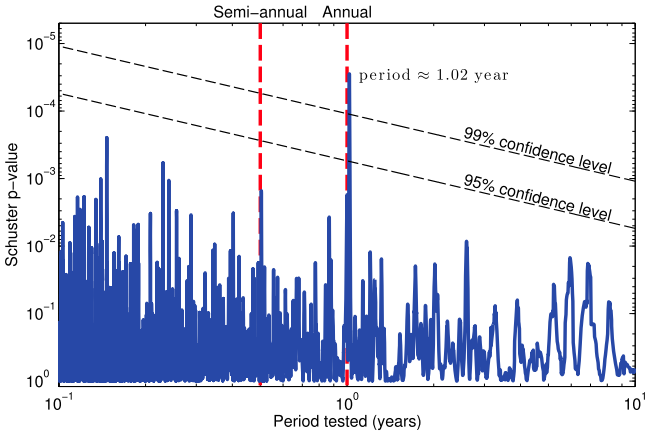

Figure 2. Schuster spectrum of large ($M_w \geq 7.0$) deep-focus (depth > 500 km) earthquakes. We compute p values for periods sampled densely from 0.1 year to 10 years. The 95% and 99% confidence levels as a function of period are plotted as the thin dashed lines. The only significant peak coincides with the annual period (the right thick dashed line).

is greatly reduced, although still present. Although the change in seasonality appears to occur near magnitude 7, given the relatively small number of events at larger magnitudes, it is difficult to determine this magnitude threshold with much precision or assess whether the change to seasonal behavior is gradual or abrupt.

To summarize, we observe that large ($M_w \geq 7.0$) deep-focus (>500 km) earthquakes seem 2 to 3 times more likely to occur in summer, and this seasonality is greatly reduced or absent for shallower depths or smaller events. Catalog completeness issues or detection threshold changes due to seasonal variations in noise levels do not explain this phenomenon, because $M_w 7.0$ is well above the ISC-GEM and Global CMT (GCMT) catalogs' completeness magnitudes (with the possible exception of the first 30 years of the twentieth century) [*Ekström et al.*, 2012; *Storchak et al.*, 2013; *Michael*, 2014] and also well above ambient noise levels on most global seismic stations. The ISC-GEM and GCMT catalogs have relatively consistent magnitude definitions [*Storchak et al.*, 2013; *Michael*, 2014]. Furthermore, because deep earthquake aftershock productivity is very low, there is no obvious temporal clustering among the $M_w \geq 7.0$ events that might bias the statistics. A rare exception is remote triggering of an $M > 7$ by another $M > 7$ [*Tibi et al.*, 2003; *Zhan and Shearer*, 2014], but even a conservative count presents less than five such examples, which given our sample size of 60 earthquakes will not affect our observation significantly.

3. A Post Facto Schuster Test

In the previous section, we present the observation of seasonality for large ($M_w \geq 7.0$) deep (depth > 500 km) earthquakes. The total number of such events is 60 (Table S1), 42 of which occurred in summer (from April to September). To quantify the probability of observing this level of seasonality just by random chance, and to resolve the most significant periodicities (instead of assuming period = 1 year), here we compute a Schuster spectrum [*Ader and Avouac*, 2013], which consists of many Schuster tests spanning a wide period range. Figure 2 shows the Schuster p values as a function of period, sampled densely from 0.1 year to 10 years. Instead of interpreting the p values directly as the probability of observation just by chance, *Ader and Avouac* [2013] show that the expected minimum p value, for a catalog occurring out of a uniform seismicity, depends on the catalog duration t and period T:

$$\langle \delta_m = T/t \rangle.$$

A periodicity in the catalog will thus have a significant probability if its p value is significantly lower than this expected value. For instance, a 95% confidence level can be claimed if the corresponding p value is less than $0.05 \times \langle \delta_m \rangle$, rather than simply 0.05. In Figure 2, the two black dashed lines mark the 95% and 99% confidence levels as functions of period T. While almost all the p values are below the 95% confidence level, there is a single spike above the 99% confidence level at $T = 1.02$ years. Considering the resolution using a small catalog with only 60 events, this period coincides remarkably close to the annual period of 1 year. Additionally, the 1.02 year peak is very sharp, without obvious sidelobes or peaks at unit fractions of T (e.g., semiannual period); this indicates that the periodicity is not caused by temporal earthquake clustering (e.g., aftershocks) or a periodic but nonsinusoidal seismicity rate (e.g., periodic spikes) [*Ader and Avouac*, 2013]. This is also supported by the monthly distribution of the 60 large deep events in Figure S3, which has no clear indication of asymmetry. Again, we do not observe any significant peak above the 95% confidence level in the Schuster spectrum for events smaller than magnitude 7 (Figure S2).

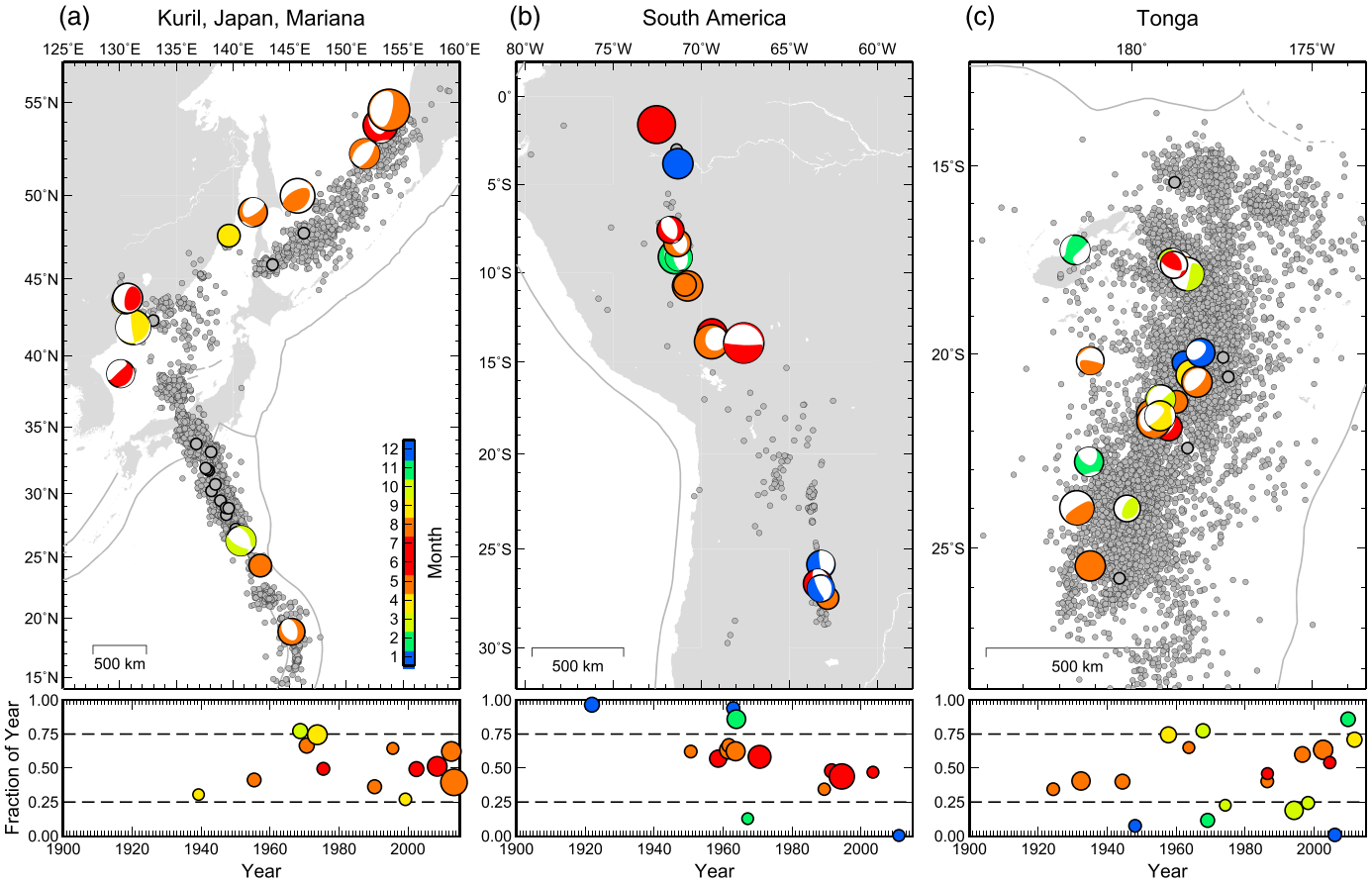

Figure 3. Regional plots of deep-focus earthquakes for the (a) NW Pacific, (b) South American, and (c) Tonga subduction zones. Events larger than 7.0 are colored by the months in which they occurred, and focal mechanisms are from the ISC-GEM or the GCMT catalogs when available. Background seismicity is shown by the small grey dots. (bottom row) Event month as a fraction of the year versus year; the two dashed lines divide the winter and summer. Symbol sizes are proportional to earthquake magnitudes.

The Schuster spectrum for large deep-focus earthquakes presents a single clean peak at ~1 year period above the 99% confidence level, which confirms our observations in the last section. However, this is exactly why the computed *p* value is biased: we first identify the seasonal pattern from the catalog and then carry out Schuster tests with the same data (i.e., data fishing) [*Gelman and Loken*, 2014; *Nuzzo*, 2014]. Therefore, we cannot have complete confidence that the observed seasonality is statistically significant. Nonetheless, we will proceed in three ways: (1) Assuming the anomaly is real and not simply due to random chance, we will try to identify more precisely where in the data the anomaly is coming from; (2) assuming the anomaly is real, we will make a specific prediction about future seasonal signals that will allow future researchers to test for significance without any bias from having already seen the data; and (3) we will discuss possible causes of a seasonal signal in deep earthquake occurrence.

4. Source Regions of the Anomaly

Identifying where the anomaly is coming from, although in terms of statistics is even closer to the data fishing approach, may help us identify possible physical reasons for the seasonality. Global deep-focus earthquakes occur almost exclusively in subduction zones (active or fossil). For the 60 large deep-focus earthquakes discussed in this paper, the three largest contributors are the Tonga, northwest Pacific (Kuril, Japan, and Mariana), and South American subduction zones (Figure 3). The next two largest groups, the Philippine and Indonesia subduction zones together contributed 8 out of the 60 events and will only be discussed briefly in Figure S4.

In Figure 3, we plot the large deep-focus earthquakes' focal mechanisms when available from the ISC-GEM or the GCMT catalogs, colored by the months in which they occurred. For each subduction zone, Figure 3 (bottom row) displays the event month as a fraction of the year versus the year. Therefore, events between the two dashed lines at 0.25 and 0.75 occurred in summer. For the northwest Pacific subduction zone (Kuril, Japan, and Mariana), strikingly, 12 out of 13 events occurred in the summer time. In South America, 10 out of 15 events, or 2/3, happened in summer, which is comparable to the global average (Figure 1). Interestingly, within these two subduction zones, the three largest deep-focus earthquakes, the 31 July 1970 M_w 8.0 Colombia earthquake, 9 June 1994 M_w 8.2 Bolivia earthquake, and the 24 May 2013 M_w 8.3 Sea of Okhotsk earthquake all occurred in summer. However, large deep-focus earthquakes in the Tonga subduction zone seem to break the pattern, with only slightly more than half, 12 out of 20 events in summer. Therefore, large deep-focus earthquakes in the Northwestern Pacific and South American subduction zones are the strongest sources of the observed seasonality. We do not observe any obvious dependence on the focal mechanisms.

The Tonga subduction zone has long been known to be special for deep earthquakes. Based on the U.S. Geological Survey Preliminary Determination of Epicenters (PDE) earthquake catalog, Tonga accounts for about 68% of the global deep-focus seismicity. In Figure 3c, when we display these smaller events as grey dots in the background, the large events in color are essentially embedded within a cloud of smaller events. In contrast, the Northwestern Pacific and South American subduction zones only contribute 16% and 2% of the global deep-focus seismicity, respectively. However, the three subduction zones' productivities of large events are far from proportional but comparable, which reflects possible variations in earthquake *b* values [*Giardini*, 1988; *Frohlich and Davis*, 1993; *Wiens and Gilbert*, 1996; *Kagan*, 1999; *Wiens*, 2001]. Furthermore, large deep-focus earthquakes in Figures 3a and 3b tend to be more isolated from the neighboring seismicity [*Kirby et al*., 1991, 1996; *Frohlich*, 2006]. This pattern is very clear for the South American subduction zone without much background seismicity (Figure 3b) but also intriguing for the northwest Pacific subduction zone with moderate background seismicity: most large events occurred on the edges of the Wadati-Benioff zone. For example, the 2013 M_w 8.3 Sea of Okhotsk earthquakes occurred in a corner region with significantly lower background seismicity than the neighboring regions [*Zhan et al*., 2014]. This is consistent with the observations made by *Kirby et al*. [1996]. Finally, regional analyses of smaller deep earthquakes (e.g., $6.0 < M_w < 7.0$) in the NW Pacific, South American, and Tonga subduction zones do not show seasonality, despite the regional differences observed for the larger events.

In summary, the seasonal pattern seems strongest among earthquakes in the northwest Pacific and South American subduction zones and relatively weak in the Tonga subduction zone. The large summer events also tend to be isolated from the neighboring seismicity. However, we will not present more Schuster tests for subsets of the data (with different choices of magnitude threshold, regions, and depth ranges), because the data fishing issue is likely even stronger in this case.

5. Prediction About Future Deep Earthquakes

We find the observed seasonality for large deep-focus earthquakes intriguing, but meanwhile, due to data selection criteria and the related data fishing issue, we cannot have complete confidence that the observed seasonality is statistically significant. Therefore, in this section, we discuss specific data selection criteria and statistical procedures to test the hypotheses when new data become available in the future. We also compute when we will likely be able to validate or falsify the proposed deep earthquake seasonality. This has some precedent in seismology [for example, *Savage and Cockerham*, 1987], noting apparent periodicity in large earthquakes near Mammoth Lakes, California, made a testable prediction about a future event, which was later falsified.

We first confine future data to a subset in which we believe the seasonality is the strongest: large ($M \geq 7.0$) earthquakes deeper than 500 km in the Northwestern Pacific (including Kuril, Japan, and Mariana) and South American subduction zones (regions shown in Figures 3a and 3b). For this data set, we estimate that the probability of summer events is 2 to 3 times higher than winter events; i.e., the expected fraction of events in summer is 2/3 to 3/4. However, because of the data fishing issue, we cannot have confidence that the true probability of summer events is nearly this high. To account for this, our most conservative hypothesis is only that the true probability of summer events is larger than 1/2; i.e., we do not require that the rate be as high as that observed in the past.

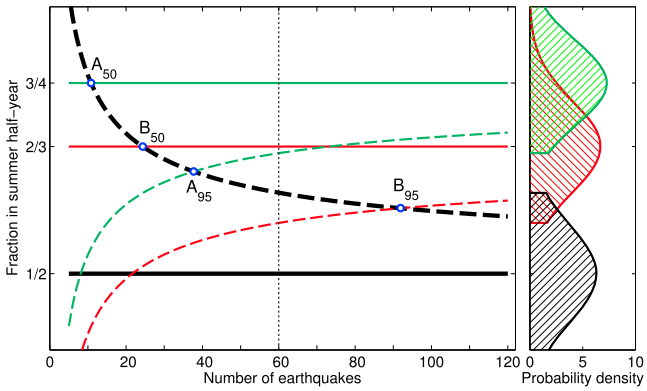

Figure 4. (left and right) Predictions about future large deep-focus earthquakes. Horizontal lines show various assumed fractions (1/2, 2/3, and 3/4) in the summer half year, and the dashed lines plot the upper (for 1/2, in black) or lower (for 2/3 and 3/4, in red and green) 95% confidence limits, respectively, as a function of the number of earthquakes. A_{50}, A_{95}, B_{50}, and B_{95} are cross points indicating specific chances to reject the null hypothesis with 95% confidence. Figure 4 (right) displays the probability density functions for the case of 60 events, along the vertical dashed line in Figure 4 (left). The cutoffs on the Gaussian functions show the upper or lower 95% confidence limits.

Under these conditions, the null hypothesis to reject is that earthquake occurrence is random and Poissonian, in which case there is no true difference between the summer and winter rates and the expected fraction of summer events is 1/2. In Figure 4, we show the expected distributions and χ^2 95% confidence limits for various assumed underlying summer month probabilities, as a function of the total number of earthquakes. The thick solid black line plots the null hypothesis of a 50% summer event rate, and the thick dashed black line shows the upper 95% confidence limit. The null hypothesis can be rejected with 95% confidence if the observed summer fraction falls above this dashed line. For example, our current data set consists of 60 earthquakes, marked by the vertical thin dotted line in Figure 4. A profile of the probability density function along the dashed line is shown in Figure 4 (right) in black. The area of the black shadow below the top edge of the Gaussian function equals 0.95; a summer fraction above the top edge (e.g., 2/3 to 3/4 in our observations) therefore falls well beyond the 95% confidence limit and would be considered statistically significant in the absence of the data fishing issue. In Figure 4 (left), the thick dashed line approaches the expected value as the number of samples increases because random fluctuations tend to average out and it becomes less likely that large differences in rate would occur.

Assuming the seasonality is real, the likely length of time required to reject the null hypothesis depends upon the true summer event fraction. For example, if the true mean is 3/4, there is 50% chance that a particular observation falls above the green line in Figure 4. Therefore, the cross-point A_{50} between the green line and the black dashed line indicates that we need ~11 samples to have a 50% chance to reject the null hypothesis with 95% confidence. To have a better chance, we need more events. For example there is a 95% chance that the observation falls above the green dashed line, for a true mean of 3/4. Then the cross-point A_{95} shows that we need about 38 samples to have 95% chance to reject the null hypothesis with 95% confidence. This relation is also illustrated by the nonoverlapping black and green Gaussian functions for 60 samples in Figure 4 (right). Similarly, if the true mean summer fraction is 2/3, B_{50} and B_{95} show that we need 25 or 92 events to have a 50% or 95% chance, respectively, to reject the null hypothesis with 95% confidence. On the other hand, Figure 4 also shows how to falsify seasonal hypotheses with a specific summer fraction. For example, A_{95} can be interpreted as how many samples we need to have a 95% chance to reject a 3/4 summer fraction hypothesis with 95% confidence, if the true summer fraction mean is 1/2 (no seasonality).

The average rate for large deep-focus earthquakes in the past is just one event per 2 to 3 years, with significant fluctuations (e.g., an earthquake drought between 1976 and 1984). Therefore, even if the average rate continues, we probably will need to wait for several decades or longer to confirm deep earthquake seasonality or falsify specific predictions of its strength. But at least we are able to make testable hypotheses for future seismologists to evaluate.

6. Possible Physical Causes of Deep Earthquake Seasonality

Two possible physical causes of the observed seasonality are the annual solar tide and the annual pole tide due to polar motions. However, these seem improbable causes because the stress from these two tides is very small (<1 KPa) compared with other tidal stresses (e.g., 12 h and 24 h lunar tides and semiannual solar tide)

[*Agnew*, 2007]. Furthermore, we do not observe periodicity due to the "nearby" and relatively strong semi-annual solar tide and 14 month pole tide (Figure 2). These results seem to suggest that if the seasonality exists, it must have a narrow response band near the 1 year period. Although a similarly narrow response band has been observed in the Himalaya "subduction zone" [*Ader and Avouac*, 2013] and reproduced in numerical experiments using rate-state friction laws [*Ader et al*., 2014], this can plausibly be attributed to seasonal changes in surface loading, which is unlikely to be a factor for deep earthquakes. Our understanding of deep earthquake mechanisms is still too limited to infer their nucleation timescales. As presented above in section 4, we noticed that large deep-focus earthquakes in summer tend to be isolated from the neighboring seismicity. It has been proposed that these large isolated earthquakes occurred in highly stressed regions that may have difficulty in nucleating [*Kirby et al*., 1996; *Frohlich*, 2006]. These regions, therefore, may be more susceptible to stress perturbations, such as tidal stresses. Once triggered/initiated, the rupture will grow to the maximum possible size [*Kirby et al*., 1996], which may explain why we do not observe seasonality in smaller earthquakes. Finally, the depth range ($>$500 km) in which we observe seasonality coincides with the depth range ($>$550 km) inferred to have sharper and simpler earthquakes, in terms of source duration functions, than in shallower depths [*Persh and Houston*, 2004; *Tocheport et al*., 2007]. Deep earthquakes at this depth range may require a different mechanism [*Houston*, 2007]. From a Bayesian point of view, the speculative nature of the possible mechanisms discussed here reduces the likelihood that we are seeing a real signal, as does the fact that the seasonality is not seen for smaller, more numerous earthquakes. Nonetheless, if our prediction in section 5 is confirmed, then there must be a physical cause, and our discussions in this section should be interpreted in that context.

7. Conclusions

Since Conrad's paper in 1933 [*Conrad*, 1933], there have been many attempts to observe earthquake periodicity but most prove unreliable after more careful statistical tests. Here using a combined catalog (ISC-GEM + GCMT) from 1900 to the present, we report new possible evidence for seasonality in large deep-focus earthquakes. Of 60 events with magnitude $\geq$ 7.0 and depth $>$ 500 km, 42 have occurred in the middle half of each year. The seasonality appears strongest in the northwest Pacific and South American subduction zones, and weakest in the Tonga region. Although the seasonal signal is very strong in $M \geq 7$ earthquakes, because of the data fishing problem, we cannot be sure the result is statistically significant. Furthermore, our limited understanding of deep earthquake mechanics, especially their nucleation and rupture mechanisms, limits our ability to identify possible causes for the seasonality. Therefore, besides waiting for more large deep-focus earthquakes to test our predictions, we encourage further study of the deep earthquake nucleation and rupture processes, including the physical conditions near hypocenters and any possible sensitivity to periodic stress perturbations.

Acknowledgments

This ISC-GEM Global Instrumental Earthquake Catalogue (1900–2009) is freely available at http://www.isc.ac.uk/iscgem/. The Global CMT catalog is freely available at http://www.globalcmt.org/. We thank Debi Kilb, Duncan Agnew, and Clifford Frohlich for their discussions and comments on an earlier version of the manuscript. We thank Douglas Wiens and the anonymous reviewer for their helpful comments. This work was supported by National Science Foundation grant EAR-111111.

The Editor thanks Douglas A. Wiens and an anonymous reviewer for their assistance in evaluating this paper.

References

Ader, T. J., and J.-P. Avouac (2013), Detecting periodicities and declustering in earthquake catalogs using the Schuster spectrum, application to Himalayan seismicity, *Earth Planet. Sci. Lett.*, *377–378*, 97–105.

Ader, T. J., N. Lapusta, J.-P. Avouac, and J. P. Ampuero (2014), Response of rate-and-state seismogenic faults to harmonic shear-stress perturbations, *Geophys. J. Int.*, *198*(1), 385–413.

Agnew, D. C. (2007), Earth tides, in *Treatise on Geophysics: Geodesy*, edited by T. A. Herring, pp. 163–195, Elsevier, New York.

Cochran, E. S., J. E. Vidale, and S. Tanaka (2004), Earth tides can trigger shallow thrust fault earthquakes, *Science*, *306*(5699), 1164–1166.

Conrad, V. (1933), Die zeitliche Folge von Beben mit tiefem Herd, *Gerl. Beitr. Z. Geophys.*, *40*, 113–133.

Curchin, J. M., and W. D. Pennington (1987), Tidal triggering of intermediate and deep focus earthquakes, *J. Geophys. Res.*, *92*(B13), 13,957–13,967, doi:10.1029/JB092iB13p13957.

Dziewonski, A., T. A. Chou, and J. Woodhouse (1981), Determination of earthquake source parameters from waveform data for studies of global and regional seismicity, *J. Geophys. Res.*, *86*(B4), 2825–2852, doi:10.1029/JB086iB04p02825.

Ekström, G., M. Nettles, and A. Dziewoński (2012), The global CMT project 2004–2010: Centroid-moment tensors for 13,017 earthquakes, *Phys. Earth Planet. Inter.*, *200*, 1–9.

Frohlich, C. (2006), *Deep Earthquakes*, Cambridge Univ. Press, Cambridge.

Frohlich, C., and S. D. Davis (1993), Teleseismic *b* values; Or, much ado about 1.0, *J. Geophys. Res.*, *98*(B1), 631–644, doi:10.1029/92JB01891.

Gelman, A., and E. Loken (2014), The statistical crisis in science, *Am. Sci.*, *102*, 460–465.

Giardini, D. (1988), Frequency distribution and quantification of deep earthquakes, *J. Geophys. Res.*, *93*(B3), 2095–2105, doi:10.1029/JB093iB03p02095.

Green, H. W., 2nd, W. P. Chen, and M. R. Brudzinski (2010), Seismic evidence of negligible water carried below 400-km depth in subducting lithosphere, *Nature*, *467*(7317), 828–831.

Heaton, T. H. (1975), Tidal triggering of earthquakes, *Geophys. J. Int.*, *43*(2), 307–326.

Heaton, T. H. (1982), Tidal triggering of earthquakes, *Bull. Seismol. Soc. Am.*, *72*(6A), 2181–2200.

Houston, H. (2007), Deep earthquakes, in *Treatise on Geophysics*, edited by G. Schubert, pp. 321–350, Elsevier, Amsterdam.

Jeffreys, H. (1938), Aftershocks and periodicity in earthquakes, *Gerlands Beitr. Geophys.*, *53*, 111–139.

Kagan, Y. (1999), Universality of the seismic moment-frequency relation, in *Seismicity Patterns, Their Statistical Significance and Physical Meaning*, edited by M. Wyss, K. Shimazaki, and A. Ito, pp. 537–573, Springer, Basel.
Kirby, S. H., W. B. Durham, and L. A. Stern (1991), Mantle phase changes and deep-earthquake faulting in subducting lithosphere, *Science*, *252*(5003), 216–225.
Kirby, S. H., S. Stein, E. A. Okal, and D. C. Rubie (1996), Metastable mantle phase transformations and deep earthquakes in subducting oceanic lithosphere, *Rev. Geophys.*, *34*(2), 261–306, doi:10.1029/96RG01050.
Landsberg, H. (1948), Note on deep-focus earthquakes, pressure changes, and pole motion, *Geogr. Ann., Ser. A*, *12*(5–6), 177–180.
Michael, A. J. (2014), How complete is the ISC-GEM global earthquake catalog?, *Bull. Seismol. Soc. Am.*, *104*(4), 1829–1837.
Nuzzo, R. (2014), Statistical errors, *Nature*, *506*(13), 150–152.
Persh, S. E., and H. Houston (2004), Deep earthquake rupture histories determined by global stacking of broadband P waveforms, *J. Geophys. Res.*, *109*, B04311, doi:10.1029/2003JB002762.
Savage, J., and R. S. Cockerham (1987), Quasi-periodic occurrence of earthquakes in the 1978–1986 Bishop-Mammoth Lakes sequence, eastern California, *Bull. Seismol. Soc. Am.*, *77*(4), 1347–1358.
Shearer, P. M., and P. B. Stark (2012), Global risk of big earthquakes has not recently increased, *Proc. Natl. Acad. Sci. U.S.A.*, *109*(3), 717–721.
Stetson, H. T. (1935), The correlation of deep-focus earthquakes with lunar hour angle and declination, *Science*, *82*(2135), 523–524.
Storchak, D. A., D. Di Giacomo, I. Bondar, E. R. Engdahl, J. Harris, W. H. K. Lee, A. Villasenor, and P. Bormann (2013), Public release of the ISC-GEM global instrumental earthquake catalogue (1900–2009), *Seismol. Res. Lett.*, *84*(5), 810–815.
Tibi, R., D. A. Wiens, and H. Inoue (2003), Remote triggering of deep earthquakes in the 2002 Tonga sequences, *Nature*, *424*(6951), 921–925.
Tocheport, A., L. Rivera, and S. Chevrot (2007), A systematic study of source time functions and moment tensors of intermediate and deep earthquakes, *J. Geophys. Res.*, *112*, B07311, doi:10.1029/2006JB004534.
Vidale, J. E., D. C. Agnew, M. J. S. Johnston, and D. H. Oppenheimer (1998), Absence of earthquake correlation with Earth tides: An indication of high preseismic fault stress rate, *J. Geophys. Res.*, *103*(B10), 24,567–24,572, doi:10.1029/98JB00594.
Wahr, J., M. Molenaar, and F. Bryan (1998), Time variability of the Earth's gravity field: Hydrological and oceanic effects and their possible detection using GRACE, *J. Geophys. Res.*, *103*(B12), 30,205–30,229, doi:10.1029/98JB02844.
Wiens, D. A. (2001), Seismological constraints on the mechanism of deep earthquakes: Temperature dependence of deep earthquake source properties, *Phys. Earth Planet. Inter.*, *127*(1), 145–163.
Wiens, D. A., and H. J. Gilbert (1996), Effect of slab temperature on deep-earthquake aftershock productivity and magnitude-frequency relations, *Nature*, *384*(6605), 153–156.
Zhan, Z., and P. M. Shearer (2014), Dynamic triggering of deep earthquakes—A global perspective, in *AGU Fall Meeting*, edited, San Francisco, Calif.
Zhan, Z., H. Kanamori, V. C. Tsai, D. V. Helmberger, and S. Wei (2014), Rupture complexity of the 1994 Bolivia and 2013 Sea of Okhotsk deep earthquakes, *Earth Planet. Sci. Lett.*, *385*, 89–96.